Scaling of Pseudorapidity Distributions at c.m. Energies up to 0.9 TeV

UA5 Collaboration

G.J. Alner[3][a], R.E. Ansorge[3], B. Åsman[5], C.N. Booth[3][d], L. Burow[1], P. Carlson[5], R.S. DeWolf[3], A. Drees[1], B. Eckart[1], G. Ekspong[5], I. Evangelou[4][c], A. Eyring[1], J.-P. Fabre[4], C. Fuglesang[5], J. Gaudaen[2][b][d], C. Geich-Gimbel[1], B. Holl[1], R. Hospes[1], D.P. Johnson[2], K. Jon-And[5], F. Lotse[5], N. Manthos[4][c], R. Meinke[1], D.J. Munday[3], J.E.V. Ovens[3], W. Pelzer[1], J.J. Reidy[4][e], J.C. Rushbrooke[3], H. Schmickler[1], F. Triantis[4][c], L. Van hamme[2], C. Walck[5], C.P. Ward[3], D.R. Ward[3], C.J.S. Webber[3], T.O. White[3], G. Wilquet[2], N. Yamdagni[5]

[1] Physikalisches Institut der Universität D-5300 Bonn, Federal Republic of Germany
[2] Inter-University Institute for High Energies (ULB-VUB), B-1 C Brussels, Belgium
[3] Cavendish Laboratory, Department of Physics, University, Cambridge, CB3 OHE, UK
[4] CERN, Geneva, Switzerland
[5] Institute of Physics, University, S-113 46 Stockholm, Sweden

Abstract. New data are presented on charged particle pseudorapidity distributions for inelastic events produced at c.m. energies $\sqrt{s} = 200$ and 900 GeV. The data were obtained at the CERN antiproton-proton Collider operated in a new pulsed mode. The rise of the central density $\rho(0)$ at energies up to $\sqrt{s} = 900$ GeV has been studied. A new form of central region scaling is found involving the density $\rho_n(0)$ for charged multiplicity n, namely that the scaled central density $\rho_n(0)/\rho(0)$ expressed as a function of $z = n/\langle n \rangle$ is independent of s. Scaling in the fragmentation region holds to 10–20%, and the small amount of scale-breaking observed here could be accommodated within the framework suggested by Wdowcyk and Wolfendale to account for both accelerator and cosmic ray data.

Introduction

A study of hadron-hadron collisions at the highest energies has revealed many regularities that could shed light on the underlying dynamics. The data [1, 2] up to a c.m. energy ($\sqrt{s}$) of 546 GeV reveal a steady rise with energy of the charged particle density in the central region near $x = 0$ (where $x = p_L^*/p_{max}^*$ as measured in the c.m.s), violating so-called Feynman scaling [3]. Whether there is scaling in the fragmentation region (usually taken to mean $|x| \gtrsim 0.05$) is, on the other hand, an open question, whose resolution is important for models and for an understanding [4, 5] of cosmic ray cross-section measurements at $\sqrt{s} \sim 1$ TeV and beyond.

A measure of particle density can be obtained in terms of the rapidity of each produced particle, which can be approximated by the pseudorapidity ($\eta = -\ln \tan \theta/2$) depending only on the c.m. production angle θ. In this letter we report on new measurements of the pseudo-rapidity distributions at c.m. energies of 200 and 900 GeV, the latter being the highest energy accelerator data so far presented. The data are based on 3,500 (2,100) fully reconstructed events at 900 (200) GeV from a run at the CERN Collider during its operation in pulsed mode in March-April 1985. Details on the performance of the accelerator and other running conditions are given in [6].

Experimental Details

The UA5 detector and event analysis procudures are described elsewhere [7, 8, 9]. Two large streamer

chambers, $6 \text{ m} \times 1.25 \text{ m} \times 0.5 \text{ m}$, where placed above and below the SPS beryllium beam pipe. This gave a geometrical acceptance of about 95% for $|\eta| < 3$, falling to zero at $|\eta| = 5$. The chambers were triggered by requiring one or more hits in scintillation counter hodoscopes at each end of the chambers covering $2 < |\eta| < 5.6$. Two triggers were taken in parallel: a "2-arm" trigger requiring hits at both ends to select mainly non single-diffractive (NSD) events, and a "1-arm" trigger demanding a hit in only one arm to select highly asymmetric events of the type $\bar{p} + p \rightarrow X + p^\star$ such as single diffractive (SD) events. Monte Carlo simulations were used to estimate that the 2-arm trigger accepted 95% (91%) of the NSD cross section at 900 (200) GeV, and to correct for those NSD events that were missed. By combining 1-arm and 2-arm data we obtained a sample pertaining to the inelastic (i.e. NSD + SD) cross-section with 93% (95%) efficiency, the losses again being corrected for by using the Monte Carlo. Distributions for both the NSD and inelastic samples are presented below.

The methods by which streamer chamber tracks were measured, geometrically reconstructed, and associated with primary or secondary vertices are as explained in [7, 8]. The observed pseudorapidity distributions were corrected using Monte Carlo simulations. The event generator in the simulation program was tuned so as to reproduce correctly the observed features of particle production at 546 GeV: multiplicity and rapidity distributions [7, 10], observed yields of strange particles and baryons [11–13] and of photons [14]. The results were then parametrized as a function of c.m. energy [15, 8, 11], and calculations performed at 200 and 900 GeV. Further tuning was then performed in respect of multiplicity and rapidity distributions using early 900 GeV data already analysed [9, 16]. Produced particles were tracked through the detector allowing for interactions and scattering. Measurement errors were taken into account. The 10,000 simulated events were then used to determine the efficiency of the 1-arm and 2-arm triggers, and the effects of geometrical acceptance losses and residual contamination of primary tracks by secondaries [8]. The outcome was an estimate of the efficiency $\varepsilon_n(\eta)$ for observing tracks as a function of η and charged multiplicity n for each of the event categories NSD and inelastic, and these were used to obtain corrected pseudorapidity distributions from observed ones.

---

* Because of the background from the more intense proton bunch the other 1-arm trigger, yielding events of type $\bar{p} + p \rightarrow \bar{p} + X$, was not used

Results

Figures 1a and b show the distributions $\rho(\eta) = \frac{1}{\sigma} \frac{d\sigma}{d\eta}$, for NSD and inelastic events respectively, at 53, 200, 546 and 900 GeV. The 53 GeV data [17] were from an earlier run with the UA5 detector at the ISR, where similar analysis procedures were used. Likewise the 546 GeV data were from the 1982 UA5 Collider run [8]. The fact that the data at all four energies came from the same detector using the same analysis methods obviously means that comparisons between energies are more reliable. Figures 1a, b show that whereas the available rapidity range ($Y_{\text{beam}} = \ln \frac{\sqrt{s}}{m_{\text{proton}}}$) has extended by about 72% in going from 53 GeV (4 units) to 900 GeV (6.9 units), the width of the distribution has only increased by about 50%. There is a continuing steady rise in the central value $\rho(0)$, as shown in Fig. 2, which includes data from from ISR [18] and Fermilab [19]. The inelastic values of $\rho(0)$ above $\sqrt{s} = 15$ GeV can be fitted to either a $\ln s$ or power law dependence on energy, viz

$$\rho(0) = (0.01 \pm 0.14) + (0.22 \pm 0.02) \ln s \quad (\chi^2/\text{NDF} = 6.0/7)$$
$$= (0.74 \pm 0.04) s^{(0.105 \pm 0.006)} (\chi^2/\text{NDF} = 4.8/7).$$

These fits are shown as curves on Fig. 2.

Figures 3a and b show the distributions $\rho_n(\eta) = \frac{1}{\sigma_n} \cdot \frac{d\sigma_n}{d\eta}$ in different intervals of charged multiplicity n for NSD events at 200 and 900 GeV. At fixed n, $\rho_n(0)$ is falling with increasing $\sqrt{s}$, and the $\rho_n(\eta)$ distributions are getting broader. The values of $\rho_n(0)$ are plotted against n for 200, 546 and 900 GeV in Fig. 4a. Figure 4b shows values of the ratio of $\rho_n(0)$ at the same n for two pairs of energies. Naively one would expect $\rho_n(0)$ to scale like $1/Y_{\text{beam}}$ for fixed n, but instead of $\rho_n^{900}(0)/\rho_n^{546}(0) = 0.92$ and $\rho_n^{900}(0)/\rho_n^{200}(0) = 0.78$ as expected, one finds experimental values of (0.88 ± 0.01) and (0.71 ± 0.01) respectively. Figure (4a) also shows that at fixed energy $\rho_n(0)$ is rising faster than n, meaning that distributions are getting narrower with n. Despite these tendencies, we see in Fig. 4c the result of plotting against $z = n/\langle n \rangle$ values of $\rho_n(0)$ divided by the overall central density $\rho(0) = \sum P_n \rho_n(0)$, where $P_n = \sigma_n/\sigma$; within errors the points for different energies interpolate one another. The inset which uses a logarithmic scale for the ordinate shows how remarkably good this result is for low values of z where the error bars are too small to show on Fig. 4c. This would appear to be a new form of scaling in the central region of pseudorapidity.
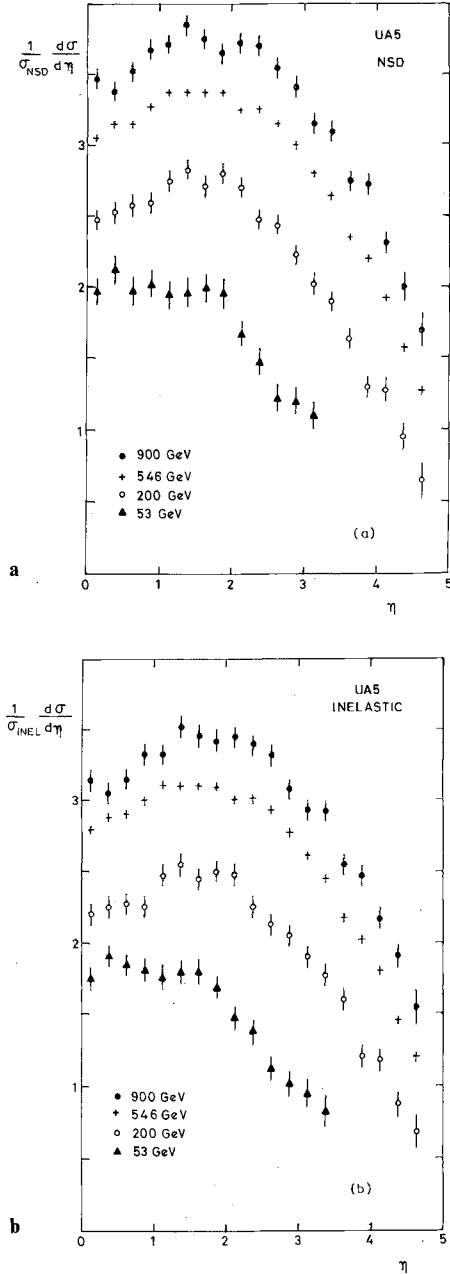
Fig. 1a, b. Pseudorapidity distributions obtained by UA5 at various energies from the ISR and the CERN Collider for **a** non single-diffractive (NSD) events, **b** inelastic (i.e. NSD+SD) events
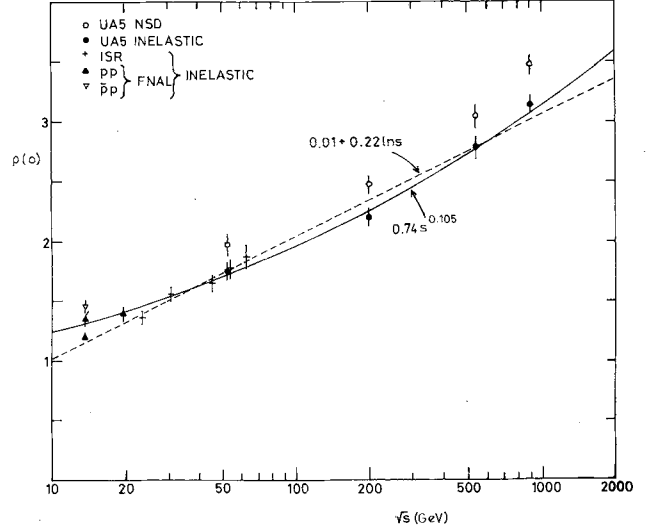

Fig. 2. Central density $\rho(0) = \dfrac{1}{\sigma}\dfrac{d\sigma}{d\eta}\Big|_{\eta=0}$ plotted as a function of c.m. energy for data from Fermilab to Collider energies. Fits to inelastic data using a linear dependence in ln s or power law dependence on s are shown
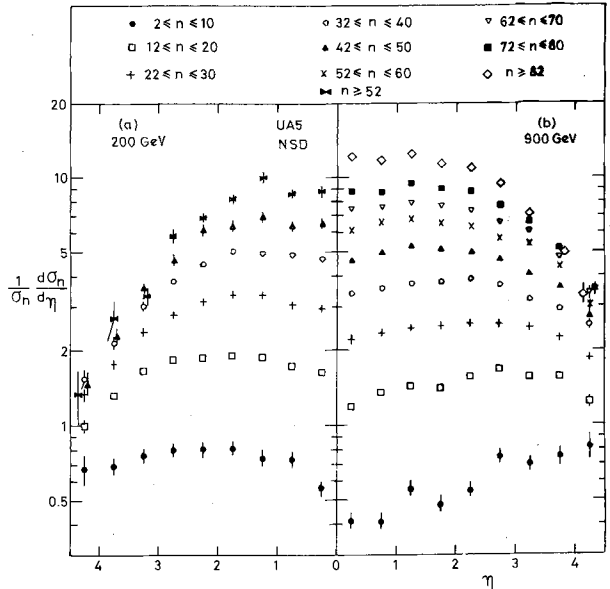

Fig. 3a, b. Pseudorapidity distributions in various intervals of charged multiplicity n for NSD events at **a** 200 GeV and **b** 900 GeV

Finally we turn to the question of scaling in the fragmentation region, $|x| \gtrsim 0.05$. Unfortunately, we do not have data in terms of the x-variable itself. Data for the inclusive processes $pp \to \pi^{\pm} X$ at laboratory momenta up to 300 GeV/c showed [20] scaling to $\pm 10\%$ in the laboratory rapidity variable, y_{lab}, for $y_{\mathrm{lab}} \lesssim 1.0$. However, for charged particle production

at the ISR ($\sqrt{s} = 30.8$ to 53.2 GeV) there was good evidence [21] for fragmentation region scaling in the pseudorapidity variable η. In terms of rapidity, fragmentation region scaling would require $\dfrac{1}{\sigma}\dfrac{d\sigma}{dy}$ to have an energy independent shape when expressed as a function of $y_{\mathrm{beam}} = y_{\mathrm{cms}} - Y_{\mathrm{beam}}$, where Y_{beam}
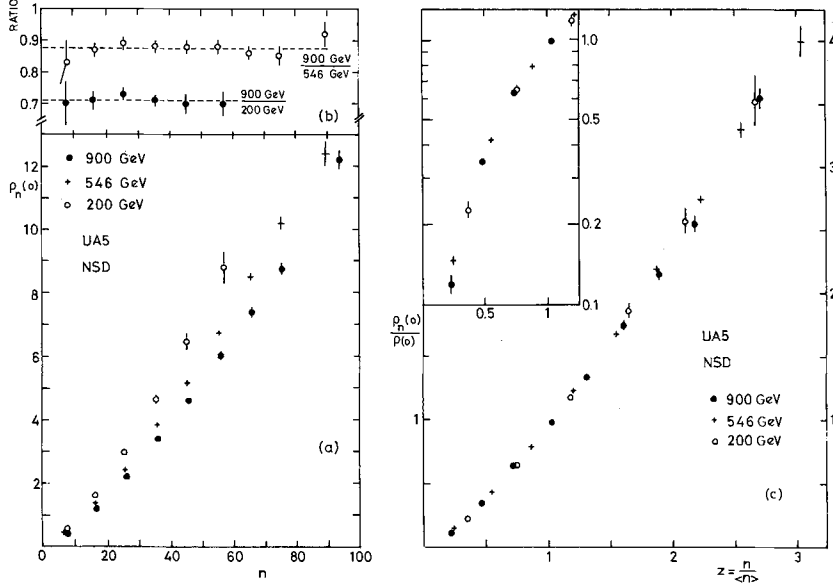
Fig. 4. a Central rapidity density $\rho_n(0)$ plotted as a function of charged multiplicity n for Collider NSD data at 200, 546 and 900 GeV. **b** Values of ratio of $\rho_n(0)$ at two pairs of energies as shown plotted against n. The dashed lines indicate mean values. **c** Plot of the scaled central density $\rho_n(0)/\rho(0)$ against $z = n/\langle n\rangle$ for Collider data at 200, 546 and 900 GeV. The inset shows on a logarithmic scale the values for small values of z

$=\ln\dfrac{\sqrt{s}}{m_{\text{proton}}}$, in a region $y_{\text{beam}}\gtrsim -2.5^\star$. In Fig. 5 we show $\dfrac{1}{\sigma}\dfrac{d\sigma}{d\eta}$ plotted against y_{beam}, taken to be $\eta - Y_{\text{beam}}$, for inelastic data in the range $\sqrt{s}=53$ to 900 GeV. Fragmentation region scaling holds to 10–20%. Therefore one simple description of the data is a steady energy-independent rise with the variable y_{beam}, until the energy-dependent plateau height given by Fig. 2 is reached. However, some slight trend towards lower values of y_{beam} for the same value of $\dfrac{1}{\sigma}\dfrac{d\sigma}{d\eta}$ as s increases may be discernible, indicative of some scale breaking.

An interpretation of both accelerator and cosmic ray data [4, 5, 22–25] has already led to the view that a substantial scale-breaking of the invariant cross section for single particle production is occurring. Wdowczyk and Wolfendale [4, 22, 23] have suggested that scaling violations in the fragmentation region may be linked to the well-known violations in the central region. They have proposed that x be replaced as the scaling variable by $x\left(\dfrac{s}{s_0}\right)^\alpha$, so that Feynman scaling would become

$$\dfrac{2E}{\sqrt{s}}\dfrac{1}{\sigma}\dfrac{d^2\sigma}{dx\,dp_T^2}=k(s,s_0)\left(\dfrac{s}{s_0}\right)^\alpha f\left\{x\left(\dfrac{s}{s_0}\right)^\alpha, p_T\right\}. \qquad (1)$$

$\star$ To see this, note that $|x|\gtrsim 0.05$ implies $\dfrac{1}{2}e^y \sim \sinh y$

$=\dfrac{P_L}{\mu}\gtrsim\dfrac{0.05\sqrt{s}}{2\mu}$, where $\mu=(p_T^2+m^2)^{1/2}$. At 200 GeV, $\langle\mu\rangle\approx\langle p_T\rangle$ $=0.39$ GeV and so $y\gtrsim 3.2$, and hence $y_{\text{beam}}\gtrsim -2.2$

The inelasticity factor $k(s,s_0)$ is intended to allow [23] for a reducing fraction of the c.m. energy going into charged particle production as s increases. Equation (1) would lead in the central region to an increase of $\rho(0)$ proportional to $k(s,s_0)\left(\dfrac{s}{s_0}\right)^\alpha$. The data of Fig. 2 showed a dependence of $\rho(0)$ on energy like $s^{0.105}$, which suggests we take $k(s,s_0)\left(\dfrac{s}{s_0}\right)^\alpha\sim\left(\dfrac{s}{s_0}\right)^{\alpha'}$.

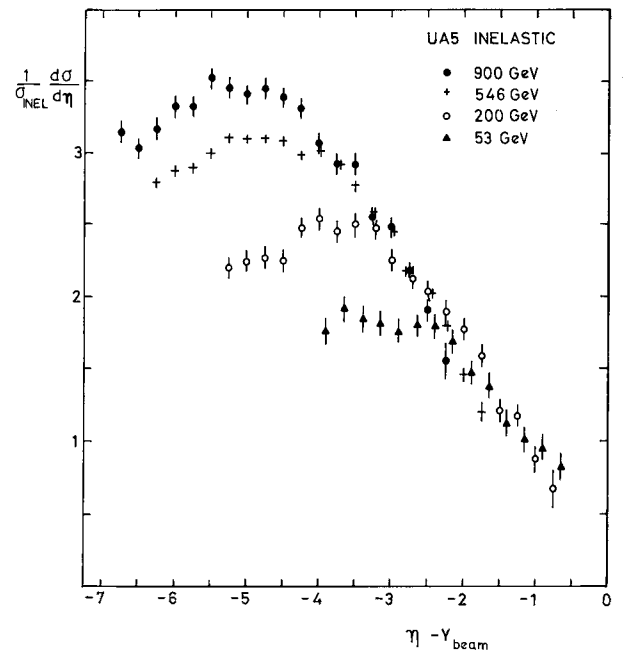**Fig. 5.** Pseudorapidity density for inelastic events plotted against $y_{\text{beam}}=\eta-Y_{\text{beam}}$ as a test of scaling in the fragmentation region, $y_{\text{beam}}\gtrsim -2.5$
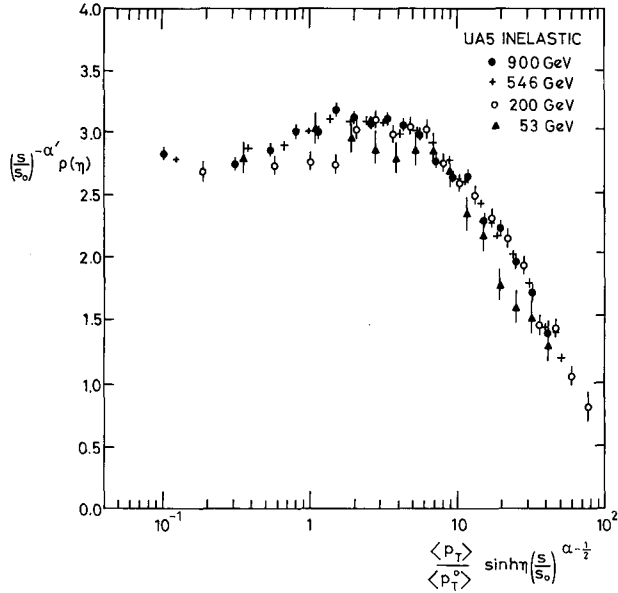
Fig. 6. Values of $\rho(\eta)\left(\dfrac{s}{s_0}\right)^{-\alpha'}$ against $\dfrac{\langle p_T\rangle}{\langle p_T^0\rangle}\sinh\eta\left(\dfrac{s}{s_0}\right)^{\alpha-1/2}$, where $\alpha=0.25\pm0.02$ and $\alpha'=0.110\pm0.005$ result from a two parameter fit to the data shown. The reference energy $\sqrt{s_0}$ is 546 GeV, and empirical values [26, 27] of$\langle p_T\rangle$ have been used

To compare (1) with our high energy data it must be transformed into dependence on the pseudorapidity variable and integrated over transverse momentum. In the Appendix we show how this can lead to the following conjecture concerning beam fragmentation region scaling, namely that $\dfrac{1}{\sigma}\dfrac{d\sigma}{d\eta}\left(\dfrac{s}{s_0}\right)^{-\alpha'}$ is independent of s when expressed as a function of the new scaling variable $\dfrac{\langle p_T\rangle}{\langle p_T^0\rangle}\sinh\eta\left(\dfrac{s}{s_0}\right)^{\alpha-1/2}$. To test this conjecture we take experimental values of $\langle p_T\rangle$ for charged particles to be 0.38 GeV/c at 53 GeV [26], and 0.39, 0.425 ($\equiv\langle p_T^0\rangle$) and 0.446 GeV/c at 200, 546 and 900 GeV respectively [27]. The two parameters α and α' were then adjusted so that the data points at 53, 200 and 900 GeV lay as close as possible to the values at the reference energy $\sqrt{s_0}=546$ GeV. We note that at this reference energy the scaling variable is just $\sinh\eta$. The result of this two-parameter fit, with $\chi^2/\mathrm{NDF}=80/47$, was the values $\alpha=0.25\pm0.02$ and $\alpha'=0.110\pm0.005$ and the plot shown as Fig. 6. Scaling appears to be quite good over the whole range 0.01–100 of this new scaling variable, and particularly good for the beam fragmentation region ($\sinh\eta\gtrsim10$) for data over the whole Collider range 200–900 GeV. We note that this fit requires that the inelsticity parameter $k(s, s_0)\sim s^{\alpha'-\alpha}=s^{-(0.14\pm0.02)}$. A recent analysis [28]

of charged particle multiplicity distributions up to Collider energies found that $k(546\ \mathrm{GeV})/k(63\ \mathrm{GeV})=0.60\pm0.06$, while we would obtain the value 0.55 ± 0.05. This consistency may lend credibility to the ad hoc formulation of (1) and (A5).

Summary

New $p\bar p$ data up to $\sqrt{s}=900$ GeV show a continuation of a power law rise with s of the central rapidity density $\rho(0)$. They also reveal a new form of central rapidity region scaling in which the scaled central density $\rho_n(0)/\rho(0)$ expressed as a function of $z=n/\langle n\rangle$ is independent of s. Scaling in the fragmentation region holds to 10–20% in terms of the pseudorapidity variable, and the small amount of scale breaking observed here can be accommodated within the framework of Wdowczyk and Wolfendale based upon an inelasticity and $\langle p_T\rangle$ changing with s and the scaling variable $x\left(\dfrac{s}{s_0}\right)^\alpha$.

Appendix

The invariant single particle cross section (1) can be written

$$\frac{1}{\sigma}\frac{d^2\sigma}{dy\,dp_T^2}=\left(\frac{s}{s_0}\right)^{\alpha'}f\left\{\frac{2\mu}{\sqrt{s}}\sinh y\left(\frac{s}{s_0}\right)^{\alpha},p_T\right\} \tag{A1}$$

on using $x=\dfrac{2\mu}{\sqrt{s}}\sinh y$, where $\mu=(p_T^2+m^2)^{1/2}$, and m is the mass of a charged secondary particle (assumed below to be a pion). We need to rewrite this in terms of the variables η and p_T, so we use the relation

$$\mu\sinh y=p_T\sinh\eta \tag{A2}$$

which leads to

$$\frac{1}{\sigma} \frac{d^2\sigma}{d\eta \, dp_T^2} = \left(\frac{s}{s_0}\right)^{\alpha'}$$

$$\cdot \, [p_T/(p_T^2 + m^2 \cosh^{-2}\eta)^{1/2}] f\left\{\frac{2p_T}{\sqrt{s}} \sinh\eta \left(\frac{s}{s_0}\right)^{\alpha}, p_T\right\},$$

(A3)

In the beam fragmentation region, $\eta \approx y \gtrsim 3$ (see footnote to p. 4), and so the Jacobian expression in square brackets is nearly unity except for $p_T < m \cosh^{-1}\eta$, i.e. $p_T < 0.014$ GeV/c, and so can be neglected. We thus have

$$\frac{1}{\sigma} \frac{d\sigma}{d\eta} = \left(\frac{s}{s_0}\right)^{\alpha'} \int_0^{\infty} f\left\{\frac{2p_T}{\sqrt{s}} \sinh\eta \left(\frac{s}{s_0}\right)^{\alpha}, p_T\right\} dp_T^2.$$

(A4)

In the absence of further knowledge of the function f we *conjecture* that beam fragmentation region scaling is to mean the following: namely that $\dfrac{1}{\sigma}\dfrac{d\sigma}{d\eta}\left(\dfrac{s}{s_0}\right)^{-\alpha'}$ is independent of s when expressed as a function of the new scaling variable $\dfrac{\langle p_T\rangle}{\langle p_T^0\rangle} \sinh\eta \left(\dfrac{s}{s_0}\right)^{\alpha-1/2}$, i.e.

$$\frac{1}{\sigma}\frac{d\sigma}{d\eta}\left(\frac{s}{s_0}\right)^{-\alpha'} = F\left\{\frac{\langle p_T\rangle}{\langle p_T^0\rangle} \sinh\eta \left(\frac{s}{s_0}\right)^{\alpha-1/2}\right\}.$$

(A5)

The quantity $\langle p_T^0\rangle$ is the value of $\langle p_T\rangle$ at $s = s_0$, at which energy the scaling variable is just $\sinh\eta$.

References

1. G.J. Alner et al.: Phys. Lett. 107 B, 310 (1981)
2. G. Arnison et al.: Phys. Lett. 123 B, 108 (1982)
3. R.P. Feynman: Phys. Rev. Lett. 23, 1415 (1969)
4. J. Wdowczyk, A.W. Wolfendale: Nature 306, 347 (1983); J. Phys. G 10, 257 (1983), and references therein
5. T.K. Gaisser: Phys. Lett. 100 B, 425 (1981)
6. G.J. Alner et al.: Phys. C – Particles and Fields 32, 153 (1986)
7. K. Alpgård et al.: Phys. Lett. 121 B, 209 (1983); G.J. Alner et al.: Phys. Lett. 138 B, 304 (1984)
8. G.J. Alner et al.: to be submitted to Phys. Rep.
9. G.J. Alner et al.: Phys. Lett. 167 B, 476 (1986)
10. D.R. Ward: Proc. of the 3rd Topical Workshop on Proton-Antiproton Collider Physics, Rome 1983, in CERN 83-04, p. 75
11. G.J. Alner et al.: Nucl. Phys. B 258, 505 (1985)
12. K. Alpgård et al.: Phys. Lett. 107 B, 315 (1981)
13. G.J. Alner et al.: Phys. Lett. 151 B, 309 (1985)
14. K. Alpgård et al.: Phys. Lett. 115 B, 71 (1982)
15. G.J. Alner et al.: Phys. Lett. 160 B, 199 (1985)
16. J.G. Rushbrooke: Proc. XVI Intern. Symp. on Multiparticle Dynamics 1985, Kiryat Anavim, Israel, p. 289. Singapore World Scientific
17. K. Alpgård et al.: Phys. Lett. 112 B, 183 (1982); A.R. Weidberg: Ph.D. Thesis, Univ. of Cambridge 1982
18. W. Thomé et al.: Nucl. Phys. B 129, 365 (1977)
19. C.P. Ward et al.: Nucl. Phys. B 153, 299 (1979); W.M. Morse et al.: Phys. Rev. D 15, 66 (1977); J. Whitmore et al.: Phys. Rep. 10 C, 273 (1974)
20. J. Whitmore: Phys. Rep. 10 C, 273 (1974)
21. L. Foà: Phys. Rep. 22 C, 1 (1975)
22. J. Wdowczyk, A.W. Wolfendale: Nuovo Cimento 54 A, 433 (1977)
23. J. Wdowczyk, A.W. Wolfendale: J. Phys. G.: Nucl. Phys. 10, 257 (1984)
24. T.K. Gaisser, F. Halzen: Univ. of Wisconsin-Madison preprint MAD/PH/236, 1985
25. J.G. Rushbrooke: Proc. XXI. Int. Conf. on High Energy Physics, C3-177. Paris, 1982
26. A.M. Rossi et al.: Nucl. Phys. B 84, 269 (1975) and references therein
27. F. Ceradini: Proc. of Int. Europhysics Conf. on High Energy Physics, p. 363. Bari, 1985
28. G.N. Fowler et al.: Phys. Lett. 145 B, 407 (1984); Phys. Rev. Lett. 55, 173 (1985)